SCIENTIFIC PAPERS
OF THE UNIVERSITY OF PARDUBICE
Series A
Faculty of Chemical Technology
8 (2002)

HYDRODYNAMIC BASED CALCULATION OF STEADY STATE PERMEATE FLUX IN MICROFILTRATION PROCESS

Petr Pospíšil, Petr MIKULÁŠEK[1] and Petr DOLEČEK
Department of Chemical Engineering, The University of Pardubice,
CZ–532 10 Pardubice

Received September 30, 2002

Crossflow microfiltration experiments were performed with aqueous titanium dioxide dispersions and alumina tubular membranes. Intensification effect of two-phase gas-liquid flow was studied on this system. The results of experiments show a positive effect of constant gas-liquid two-phase flow on the permeate flux values; both the immediate and steady state ones. The maximum increase in flux values up to 90 % was reached during the experiments in the slug flow regime of gas-liquid flow, which was found the most efficient regime applied during intensification experiments. The empirical model for steady state permeate flux and cake thickness prediction was developed from analysis of experimental results without gas flow. This model is based on Darcy's Law and on Mass balance over a membrane module. Dimensionless numbers covering all the basic operating conditions that influence permeate flux and cake thickness were introduced, and from their regression in the range of experimental feed concentrations final

[1] To whom correspondence should be addressed.

equations were derived. The results show good agreement between model prediction and experimental data with gas-liquid flow tested on the same apparatus.

Introduction

Crossflow microfiltration is a pressure driven membrane process separating dispersed matter in range of sizes from 0.05 to 10 μm from liquid. The principle of solid/liquid separation can be described as penetration of pure liquid through the membrane pores and deposition of solid particles on the membrane wall, which are trapped there due the pore and particle size difference. Increasing thickness of the layer of particles (cake formation) on the membrane wall creates higher resistance to permeate flow and causes the initial rapid decrease in flux. Another resistance can be added when the solid particles can pervade into the membrane pores and block them, and that is the case dealt with in this paper. In spite of many process difficulties, microfiltration separation process finds increasing use in water purification, brewing and biotechnology industries.

Wide range of flux enhancement methods have been developed and experimentally tested in recent years. Surveys of these methods are summarized in the literature [1,2]. Generally, there are three possible approaches to reducing or controlling the concentration polarization, cake formation and fouling: changes in surface characteristics of the membrane, pre-treatment of the feed, and fluid management methods.

Our attention has been aimed experimentally to gas-liquid two-phase flow (gas sparging) enhancement method and theoretically to the general shear stress based mathematical model, which could be used for the prediction of steady state permeate flux in microfiltration processes.

Use of a gas-liquid two-phase flow technique in the feed stream has been tried out during microfiltration and ultrafiltration processes in order to enhance the flux for various applications (biological treatment, drinking water production, macromolecules separation) and different membrane geometry (hollow fibre, flat sheet or tubular). The results of experiments showed in all the cases improvement of permeate flux and indicated some mechanisms acting near the membrane wall. The theoretical analysis of these actions should be the main object of following research in this area. The description of the impact of gas-liquid two-phase flow on events near the membrane wall is based on a change of hydrodynamic conditions inside the membrane module — which positively increases the wall shear stress, preventing membrane fouling and cake formation.

There are not many studies on modeling of flux for the enhanced microfiltration in papers, especially not in gas-liquid two-phase flow enhanced microfiltration. General model of Davis *et al.* [3] presents a solution for the

convective-diffusion equation governing the steady state concentration-polarization layer, where the thin stagnant filtration cake controls the resistance to the filtration. The resulting permeate flux is a function of membrane length, wall shear stress on the boundary layer, particle radius, viscosity, and feed concentration. The results are exact only in the diluted suspensions and are closed to the results of approximate solution of Romero *et al.* [4–6]. The approach of Romero *et al.* to quantify particle deposition on membrane wall uses an approximate integral model, which is satisfactory only when it is integrated across the concentration-polarization boundary layer. The authors introduced the value of *critical distance* from the entrance of the filter beyond which filtration cake is not swept and is formed as stagnant.

An accurate model that enables prediction of permeate flux during microfiltration with two-phase flow has not yet been proposed. Vera *et al.* [7] expressed steady state flux of gas-sparged microfiltration and ultrafiltration using two dimensionless numbers: a generalized shear stress number and a resistance number. Their experiments were carried out with dextran, wastewater effluent, tap water and ferric hydroxide suspensions and they achieved maximum flux enhancement of 200 %. The ultrafiltration model of Ghosh *et al.* [8] is based on a diffusion transport mechanism of permeate through the membrane surface and gives values of predicted flux lower than experimental ones. The model consisted of dividing the two-phase flow in the membrane into three zones enclosed in one gas slug.

In this paper, the gas-liquid two-phase flow intensification method used for microfiltration of titanium dioxide dispersions on tubular ceramic membrane is presented. The goal of this paper is the wall shear stress based calculation of the steady state permeate flux, derived from Darcy's Law adapted for our experimental system and from a mass balance solved by Datta *et al.* [9] The validation of this model by laboratory experiments is also presented.

Theoretical

Calculation of permeate flux from Darcy's Law is based on the knowledge of hydraulic resistance and the thickness of the filter cake, and on a knowledge of the membrane resistance. In the filtered systems, which allow penetration of particles into the membrane pores or surface pore blocking, the pore blocking resistance has to be included also. In that case

$$J_{SS} = \frac{\Delta P}{\mu_0 \left(R_M + R_{BL} + r\delta\right)} \tag{1}$$

where J_{SS} is the steady state permeate flux, ΔP is the transmembrane pressure difference, μ_0 is the solvent viscosity, δ is the cake thickness, R_M, R_{BL} and r are the membrane, blocking and hydraulic cake resistance, respectively. The membrane resistance can be determined from the pure water filtration experiment and is expressed as $R_M = \Delta P/\mu_0 J_0$. The hydraulic cake resistance is estimated using the Blake–Kozeny correlation

$$r = \frac{45\Phi_{max}^2}{a^2\left(1 - \Phi_{max}\right)^3} \tag{2}$$

where Φ_{max} is the maximum volume fraction of particles packed in the cake and a is the particle radius.

The sum of resistances to permeate flux is called total resistance, R_T, and is written as

$$R_T = R_M + R_{BL} + r\delta \tag{3}$$

or

$$R_T = R_M\left(1 + \frac{R_{BL}}{R_M}\right) + r\delta \tag{4}$$

where R_{BL}/R_M characterizes pore blocking factor, f_{BL}, that describes, from the hydraulic point of view, the amount of blocked pores when the system membrane/suspension allows pore blocking (when the curves of pore size distribution and particle size distribution overlap). Factor f_{BL} has the magnitude of zero when there is no pore blocking, and magnitude of infinity when all pores are blocked.

The result of microscopic mass balances for particles and the dispersing liquid along the creeping filter cake [9] was used by Mikulasek *et al.* [10] The steady state thickness of the cake results in the value of steady state permeate flux and is limited by operating conditions of the microfiltration process. This dynamic balance maintains steady state permeate flux and is controlled by the shear stress on the edge of the cake, which is a function of the initial shear stress on the clean membrane surface, τ. The differential equation of a mass balance adjusted by us is valid when we assume:

1. incompressible filtration cake,
2. that a cake once created in a given point of membrane does not change/move

any more.

An explicit solution for the cake thickness is

$$\frac{\partial \delta}{\partial t} + \frac{\tau}{\mu_C} \delta \frac{\partial \delta}{\partial x} = \frac{\Phi_B}{\Phi_{max} - \Phi_B} J \tag{5}$$

where Φ_B is the volume fraction of particles in the feed, μ_C is the apparent cake viscosity (calculated from the Mooney equation, $\mu_C = \mu_0 \exp[2.5\Phi_{max} \cdot 0.74 / /(0.74 - \Phi_{max})]$), x is the axis direction of membrane lenght, and t is time. In the steady state, and with flux J expressed from Eqs (1) and (4), the solution of Eq. (5) over the length of membrane, L, gives

$$\mu_0 \frac{\tau}{\mu_C} \left(\frac{\delta^2}{2} R_T - \frac{\delta^3}{3} r \right) = \frac{\Phi_B}{\Phi_{max} - \Phi_B} \Delta P L \tag{6}$$

Combination of Darcy's Law and the mass balance was validated experimentally by its own authors and by Mikulasek *et al.* [10] and gave good agreement of theoretical and experimental results. Hence, we have chosen it to create a dimensionless model to predict the cake thickness and steady state permeate flux in a microfiltration enhanced by gas-liquid two-phase flow.

The dimensionless quantities:

$$N_1 = R_{BL}/R_M = f_{BL},$$
$$N_2 = \tau/\Delta P$$

and

$$N_3 = \delta/d,$$
$$N_4 = \Delta P/\rho u^2$$

have been deduced semi-empirically from the data measured during microfiltration without intensification and plotted for various concentrations. The relations between numbers N_1 and N_2, and between N_3 and N_4, respectively, give us a general overview of the mutual influences of the operating conditions on permeate flux and cake thickness. Two mathematical equations have been found from interpretation of experimental data, and they relate the dimensionless numbers to feed concentrations expressed as volume fraction of solid particles in liquid. When the operating conditions of the microfiltration process we want to carry out are known, as well as the parameters of membrane and feed dispersion, we can predict

the cake thickness and pore blocking factor and subsequently permeate flux from Eq. (1). The equations are represented by the relationships

$$\frac{R_{BL}}{R_M} = f_{BL} = 0.0014\Phi^{0.652}\left(\frac{\tau}{\Delta P}\right)^{-0.898} \tag{7}$$

and

$$\frac{\delta}{d} = 0.0163\Phi^{0.533}\left(\frac{\Delta P}{\rho u^2}\right)^{0.0131\Phi^{-0.472}} \tag{8}$$

where d is the membrane diameter (or hydraulic diameter of the feed cross-section when the membrane is not tubular), ρ is the feed density and u is the feed flow velocity.

Experimental

The experimental apparatus is shown schematically in Fig. 1. A variable speed pump have was used to feed a dispersion to the membrane module from the temperature controlled storage tank. The pressure difference was controlled by a pressure valve placed downstream of the membrane module. The feed and gas flow velocities were measured by flowmeters and kept constant. All the operating conditions (transmembrane pressure, feed and gas flow velocities, gas flow mode) were monitored by a computer, which also logged the data relating to the mass of permeate collected, from which it calculated the value of permeate flux. Gas was sparged into the feed stream just before it entered the membrane module during the enhanced experiments. Feed flow velocities of 0.5 to 4 m s^{-1}, gas flow velocities of 0.2 to 3 m s^{-1} and transmembrane pressures of 50 to 200 kPa were studied. By systematically adjusting one parameter while maintaining the others constant, steady state permeate flux values were obtained as a function of each variable. All the experiments were conducted at a temperature of 25 ± 2 °C.

The suspension studied contained TiO_2 (Rutile) suspended at a known concentration (volume of particles/ volume of liquid) in distilled water. The concentrated suspension was supplied by Ostacolor a.s, Pardubice, Czech Republic and then diluted. The mean particle diameter was measured by a Light Scattering machine (ZetaPals, BIC, USA) and was equal to 400 nm, but the size distribution was very wide. The pH of the dispersions was not adjusted and its va-

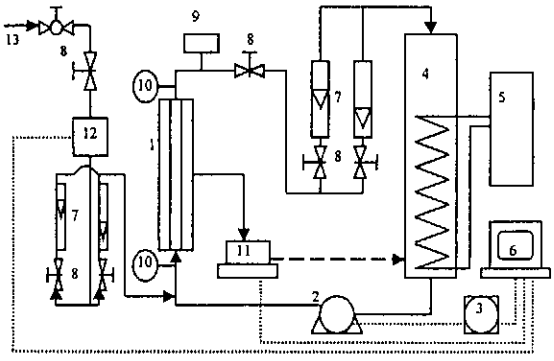

Fig. 1 Setup of experimental apparatus:1 – microfiltration module, 2 – pump, 3 – pump regulator, 4 – storage tank, 5 – thermal regulating system, 6 – computer, 7 – flowmeters, 8 – valves, 9 – pressure indicator, 10 – pressure gauge, 11– electronic balance, 12 – solenoid valve, 13 – air inlet

lue was close to 8.0.

The ceramic membranes used in this work were asymmetric, three-layered, made of alumina (produced by Terronic, Hradec Kralove, Czech Republic). They were configured as single cylindrical tubes 0.45 m long with inner diameter 6 mm and with the active surface on the inner side. The pore size distribution measured by the modified bubble test was narrow and mean pore diameter was equal to 91 nm. After every filtration, the membranes were cleaned in an ultrasonic cell and stored in dry place. They were wetted overnight before next experiment.

Results and Discussion

Membrane pure water flux and membrane resistance values were characterized by distilled water microfiltration experiments. The ceramic membrane resistance was taken as a reciprocal value of the slope of plotted pure water flux against the transmembrane pressure divided by water viscosity, from which the value of 3.33×10^{12} m^{-1} was obtained. The hydraulic cake resistance of rutile calculated using the Blake–Kozeny correlation was 1.11×10^{16} m^{-2} (the maximum volume fraction of particles packed in the cake was equal to 0.65 [10]). The analysis of the permeate showed a complete retention of the rutile in the feed, although it was possible for the particles of suspension to penetrate into the membrane pores and block them.

The experiments without gas-liquid two-phase flow confirmed the known behavior of the flux with time. The initial decrease of flux was straight and rapid and the steady state flux was reached after 1 to 2 hours — its value was about five times lower then the initial flux. Obviously, the steady state value could have been

increased, and experimentally was done so by increasing the feed flow velocity (with parallel lowering of the feed concentration or increasing the pressure difference), but this way is more energetically and investment demanding. So, there is a room for intensification methods in this process development — and we tested one of them — gas-liquid two-phase flow of the feed stream inside the tubular ceramic membrane.

Direct observations through the transparent tubular pipe of the same ID as the membranes showed that our experiments with gas-liquid two-phase flow have been later realized in the following flow patterns:

1. bubble flow — about 25 % of experiments, in the region of low gas and liquid flow velocities,
2. slug flow — about 50 % of experiments, in the region of medium gas and liquid flow velocities,
3. and churn flow — about 25 % of experiments, in the region of the highest gas and liquid flow velocities.

Previous works showed that slug flow is the most efficient regime for significant enhancement of mass transfer. The effects of gas-liquid two-phase flow on permeate flux were measured for various experimental conditions and the permeate flux obtained was always larger than that without gas flow. The presence of the gas increased the mean longitudinal velocity of the fluid, and in association with the great variations in the wall shear stress and the turbulence, it could improve the process performance. Nevertheless, the behaviour of the flux-time curves showed similar forms to those without gas flow, but the flux decline was neither so rapid nor so extreme, and the permeate flux has been maintained at a higher level during the filtering period.

The values of the normalized steady state permeate flux are plotted as a function of superficial gas flow velocity in Figs 2 and 3 for feed concentrations of 1 and 5 % v/v, respectively. There can be observed differences between the results of experiments carried out with the transmembrane pressure difference of 100 kPa and 200 kPa in Fig. 2. When the pressure of 100 kPa was applied, the increase of steady state flux compared to the same filter conditions without gas flow was quite sharp even at low gas flow velocities (increase of 50 % for u_G = 0.5 m s^{-1}). The form of the curves is independent of the superficial liquid flow velocity, and it is interesting that the plateau occurs in the regime of slug flow for gas flow velocities from 0.8 to 1.5 m s^{-1}. When the pressure of 200 kPa was applied, the increase of steady state flux was not so sharp, and above u_G = 0.5 m s^{-1} the form of the curve shows differences for various liquid flow velocities. This can be caused by more stable and compact cake deposited due to higher pressure — then the liquid flow velocity has stronger influence on cake interruption and its permeability. The intensification outcome during the experiments with dispersion of 5 % v/v shows that the impact of gas flow was similar for all the conditions applied (Fig. 3). Ge-

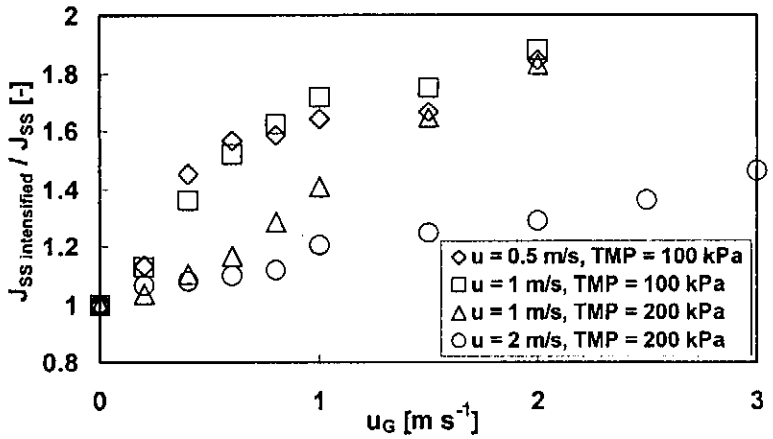

Fig. 2 Normalized steady state permeate flux as a function of the gas flow velocity for various liquid flow velocities, transmembrane pressures and feed concentration Φ_B = 0.01

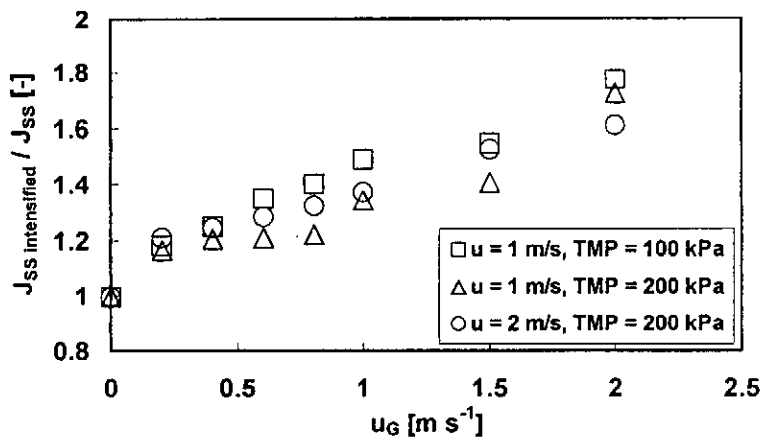

Fig. 3 Normalized steady state permeate flux as a function of the gas flow velocity for various liquid flow velocities, transmembrane pressures and feed concentration Φ_B = 0.05

nerally, the enhancement of permeate flux was the most effective when the operating conditions allowing formation of the thicker cake occurred (low feed flow velocity, high pressure).

The study of the effect of the dispersion concentration on permeate flux was undertaken by comparing the conventional single-phase cross-flow microfiltration with two-phase flow membrane system. It is interesting to note that the concentration reached with two-phase gas-liquid flow was twice as high as the

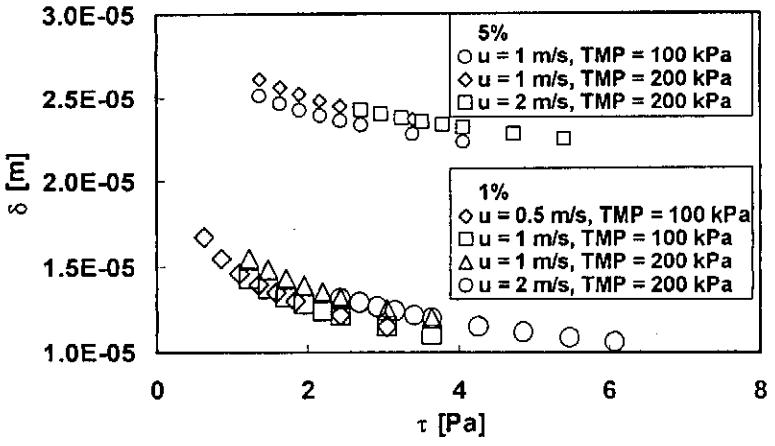

Fig. 4 Influence of wall shear stress on cake thickness for various operating conditions

concentration reached without intensification for the same filtration time. This fact can be advantageous in processes where rapid concentration of a dispersion is required. The most important consideration is that for all the concentrations in the range tested, an enhancement of the permeate flux is always observed because of the air injection. There is no concentration for which air injection has no effect on the flux.

Model Validation

After having finished the equations the validation started with calculations in this order. First, the dimensionless numbers $N_2 = \tau/\Delta P$ and $N_4 = \Delta P/\rho u^2$ were calculated for the expected conditions of microfiltration process. Values of $N_1 = R_{BL}/R_M = f_{BL}$ and $N_3 = \delta/d$ from Eqs (7) and (8) were computed for the given concentration of feed suspension, and from these numbers cake thickness and pore blocking factor were easily found. Finally, theoretical value of the steady state permeate flux was calculated from Eq. (1).

The model was validated using the sets of data from microfiltration of rutile with two-phase flow using the same microfiltration apparatus as for measurements without two-phase flow. Although the value of membrane resistance was relatively high in the case of our experimental setup, the resistance of the cake deposit and pore blocking resistance were the limiting magnitude of the steady state permeate flux reached. The hydraulic resistance of the cake is constant when calculated from the Blake–Kozeny correlation and its value changes only with the particle radius and the maximum volume fraction of particles packed in cake. So the overall cake

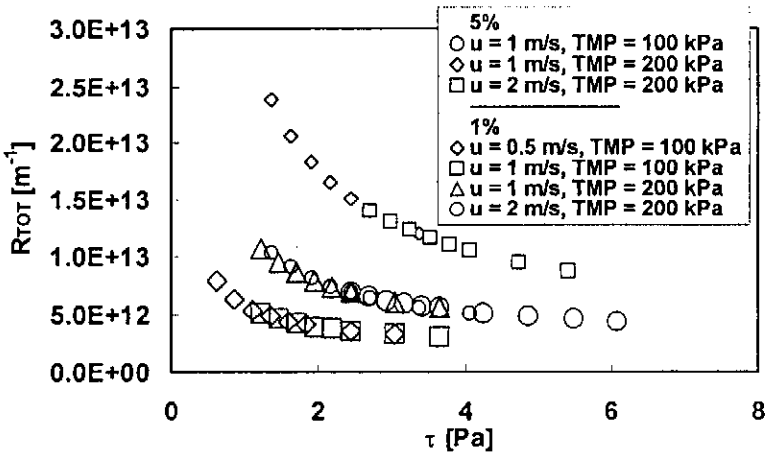

Fig. 5 Influence of wall shear stress on total resistance

resistance depended only on the cake thickness; we assumed an incompressible cake of constant porosity. When an appropriate ratio of particle size and pore diameter is chosen for the experimentation, the influence of the pore blocking resistance can be negligible. But in our system, the particle size distribution was very wide and pore blocking had to be taken into account.

Figure 4 shows the change of cake thickness with wall shear stress for various filtration conditions used during the experiments with gas flow. It can be seen that the significant effect on cake thickness was predominantly caused by concentration of the feed; it is interesting that in the range of one concentration, the decrease in cake thickness with increasing shear stress was not so important and was close to narrow and similar modification. The influence of the other operating conditions is not so obvious, however, a difference between results for various pressures can be observed. This may indicate that the value of wall shear stress calculated for clean membrane is not the same as that one which really impacts on the growing cake, because the shear stress during the cross flow microfiltration decreases to zero on the membrane wall with increasing cake thickness, and increases on the edge of the growing cake because of lowering cross-section for feed flow [11]. The line of total resistance plotted against the wall shear stress (Figure 5) shows similar behavior as the cake thickness. The magnitude of total resistance depends strongly on transmembrane pressure difference, while the influence of shear stress (connected to feed flow velocity) can be seen just inside the range of one pressure difference. It is explicit that the higher total resistance causes troubles to permeate flow when high pressure and low feed flow velocity are applied on the system. Of course, the more concentrated the filtered suspension, the higher is the total resistance.

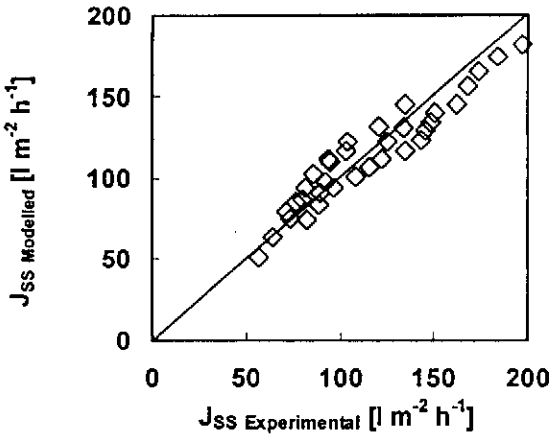

Fig. 6 Comparison of experimentally measured and calculated permeate fluxes for feed concentration Φ_B = 0.01

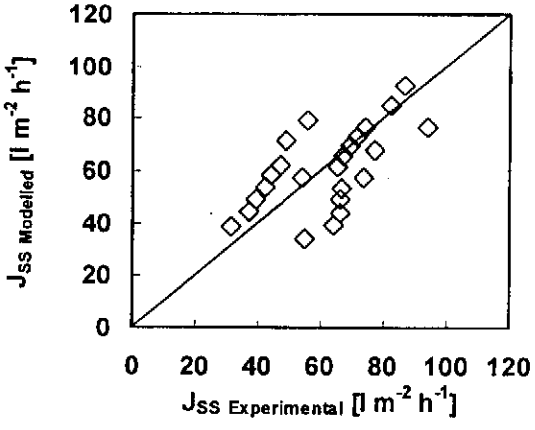

Fig. 7 Comparison of experimentally measured and calculated permeate fluxes for feed concentration Φ_B = 0.05

Figures 6 and 7 compare the values of steady state permeate flux experimentally measured and predicted by the model. Figure 6 compares the values for rutile suspension with a concentration of 1 % v/v, Fig. 7 compares values for rutile suspension with a concentration of 5 %v/v, both filtered with two-phase gas liquid flow. The quantitative agreement between theory and experiments is good, especially for a feed concentration 1 % v/v.

Variances in theoretical and experimental results can be caused by not taking into account the exact influence of overlap of particles and pores size

distributions in dimensionless numbers, and by calculating with incompressible cake.

Conclusion

The effect of superficial gas flow velocity on the steady state permeate flux improvement has been presented for various operating conditions used. The results show an increased flux in all the experiments for aqueous dispersions of titanium dioxide (rutile) that were crossflow microfiltered in a ceramic tubular membrane. A maximum flux improvement of 90 % was achieved when the operating conditions with gas flow of u_G = 2.0 m s^{-1}, a superficial feed flow velocity u = 1.0 m s^{-1}, and ΔP = 100 kPa.

A mathematical model of steady state cake thickness and permeate flux based on Darcy's Law and the Mass balance in membrane module has been presented. The empirical equations derived from microfiltration experiments without gas flow suitable for the systems where the pore blocking occurs were regressed. The validation of the model was tested on the data with two-phase gas-liquid flow with good agreement.

The difference between experimental and model results varied from:

- +20 % to -15 % for rutile of 1 % v/v,
- +45 % to -40 % for rutile of 5 % v/v.

Our simplifying presumptions of cake properties are not ideal — so they and the influence of pore and particle size distributions overlap should be taken into account in following research.

Symbols

a	particle radius, m
d	membrane tube inner diameter, m
f_{BL}	pore blocking factor
J_{SS}	steady state permeate flux, m s^{-1} (l m^{-2} h^{-1})
J_0	pure water permeate flux, m s^{-1} (l m^{-2} h^{-1})
L	membrane length, m
ΔP	transmembrane pressure difference, Pa
r	hydraulic cake resistance, m^{-2}
R_M	membrane resistance, m^{-1}
R_{BL}	pore blocking resistance, m^{-1}
R_T	total resistance, m^{-1}
t	time, s

u superficial liquid flow velocity, m s^{-1}
u_G superficial gas flow velocity, m s^{-1}
δ cake thickness, m
μ_0 permeate viscosity, Pa s
μ_C apparent viscosity, Pa s
Φ_{max} maximum volume fraction of particles packed in the cake
Φ_B volume fraction of particles in the feed
ρ feed density, kg m^{-3}
τ wall shear stress, Pa

Acknowledgements

We are grateful to the Grant Agency of the Czech Republic for providing the financial support to this research by Grant Project No. 104/00/0794.

References

[1] Mikulášek P.: Collect. Czech. Chem. Commun. **59**, 737 (1994).
[2] Wakeman R., Williams C.: Membr. Tech. **124**, 4 (2000).
[3] Davis R.H., Sherwood J.D.: Chem. Eng. Sci. **45**, 3203 (1990).
[4] Romero C.A., Davis R.H.: J. Membr. Sci. **39**, 157 (1988).
[5] . Romero C.A., Davis R.H.: Chem. Eng. Sci. **45**, 13 (1990).
[6] Romero C.A., Davis R.H.: J. Membr. Sci. **62**, 249 (1991).
[7] Vera L., Delgado S., Elmaleh S.: Chem. Eng. Sci. **55**, 3419 (2000).
[8] Ghosh R., Cui Z.F.: J. Membr. Sci. **162**, 91 (1999).
[9] Datta S., Gaddis J. L.: Sep. Sci. Tech. **32**, 327 (1997).
[10] Mikulasek P., Wakeman R.J., Marchant J.Q.: Chem. Eng. J. **69**, 53 (1998).
[11] Wakeman R.J.: Trans. IChemE. **72**, 530 (1994).